XXI IMEKO World Congress "Measurement in Research and Industry"
August 30 – September 4, 2015, Prague, Czech Republic

QUALITY CONTROL OF STRAIN GAUGES ANGULAR ORIENTATION IN STRESS TENSOR TUBES USING MACROSCOPIC VISION SYSTEM

Luís F. Lages Martins [1], *Álvaro S. Ribeiro* [1], *João Alves e Sousa* [2]

[1] National Laboratory for Civil Engineering, Lisbon, Portugal, lfmartins@lnec.pt, asribeiro@lnec.pt
[2] Regional Laboratory for Civil Engineering, Funchal, Madeira, Portugal, jasousa@lrec.pt

Abstract – This paper describes the LNEC measurement procedure of Stress Tube Tensor (STT) strain gauges angle orientation, using a macroscopic vision system, for the purpose of production quality control. Angular traceability to the International System of Units (SI) was established in the macroscopic vision system by the use of angle blocks through an internal calibration procedure also presented in this paper. The results are used to evaluate the accuracy of the STT production process.

Keywords: STT − Stress Tube Tensor, angular measurement, strain gauge, vision system.

1. INTRODUCTION

The Stress Tensor Tube (STT) is a measuring instrument with a cylindrical shape, made of a polymeric material in which several electrical strain gauges are embedded, as shown in Fig. 1. It is used for the complete determination of either the initial or the induced state of stress in rock masses and foundations by means of strain measurements made inside a borehole. It was developed by LNEC [1] and it has been widely used for several decades, contributing for experimental studies of rock masses and foundations, namely, those related to concrete dam construction scenarios [2].

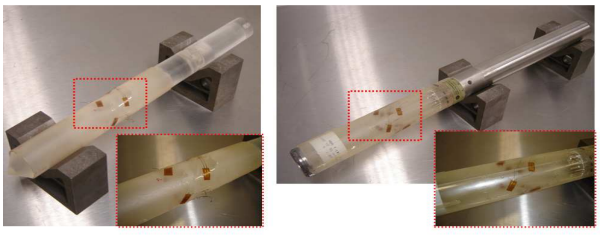

Fig. 1. Details of strain gauges location in Stress Tensor Tubes at two steps of its production.

The main steps of the stress testing procedure using STT's are presented in Figure 2, and include: (a) drill a borehole down to the neighbourhood of the position where the state of stress is to be determined; (b) drill a narrower coaxial hole at the bottom of the previous hole, in order to install and cement the STT; (c) establish an electrical connection between the STT's strain gauges and a measuring bridge on the terrain surface; (d) take the initial readings in all the strain gauges, and make an overcoring with a larger diameter while keeping the gauges connected to the measuring apparatus; (e) perform a new set of readings for each strain gauge, in order to determine deformations caused by stress relief; (f) evaluate the state of stress using a complex and multivariable mathematical model [1] (described in section 2).

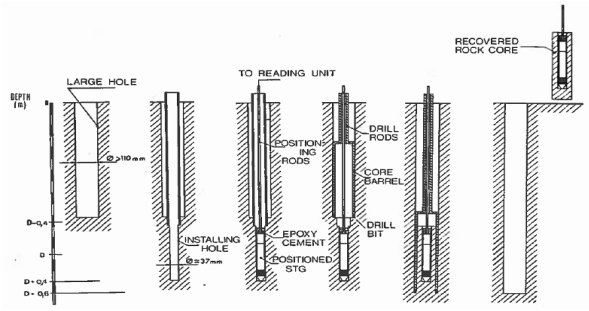

Fig. 2. Schematic representation of a field test with an STT.

The main concerns related to the technological development of the STT were focused on the following issues: (i) the number and the orientation of the strain gauges – although the stress tensor is composed by six quantities (σ_x, σ_y, σ_z, τ_{xy}, τ_{xz}, τ_{yz}) – the use of a higher number of strain gauges with different orientations is recommended as a redundancy to overcome the typical field test aggressive conditions which frequently originates failures in the STT's strain gauges; (ii) the STT dimensions which determine its stiffness and restrict laboratorial and field testing operations; (iii) the epoxy injection system used to cement the STT inside the drilled hole; (iv) the location of an additional strain gauge for temperature compensation of the strain measurements.

The LNEC's STT model is composed by 10 strain gauges aligned with axes established from the geometry of a dodecahedron or an icosahedron. These Platonic solids have 3rd order rotational symmetry in which each rotation axis passes by two opposite vertices in the case of the dodecahedron or by the centre of two opposite faces in the icosahedron. These geometrical features allow performing strain measurements in directions, non-parallel to the STT longitudinal axis, with a mutual angle of 41,81º, being a balanced geometrical configuration for the complete

determination of the stress state using any set of six strain gauges, tolerating up to four strain gauges failures.

The production process includes the manual bonding by glue of the 10 strain gauges according to a set of pairs of nominal orientation angles, α and θ, as shown in Fig. 3 [1].

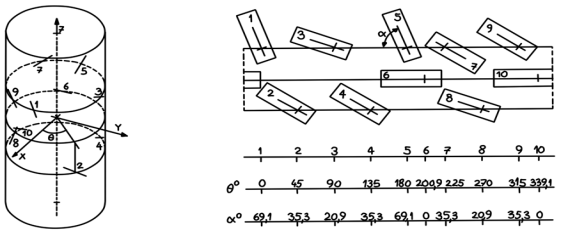

Fig. 3. Strain gauges orientations in a STT [1].

Although it is possible to use a mask to perform reference markings on the STT surface for strain gauge orientation, significant angular deviations can arise from the manual process of bonding the strain gauges, thus justifying the need to establish quality control requirements.

The use of a macroscopic vision system is considered a suitable solution for angular measurements in curved surfaces [3], as it is the case of the orientation angle α in a STT. In the absence of a rotation accessory device in the observation table, the remaining orientation angle θ can be measured by a 3D contact measuring machine. This second angular measurement is considered to be outside of the scope of this paper.

Research efforts for the establishment of SI traceability in macroscopic vision systems have been focused in dimensional features, namely, with the development of standard artefacts or optical patterns [4] where geometrical features are often not present or evaluated. This paper proposes an angular calibration method, using angular blocks, to assess the angular measurement accuracy of a specific macroscopic vision system, which is in turn used to assess the accuracy of the strain gauges angular orientation.

This study is organized in three main sections: the STT's mathematical models (section 2); the description and discussion of the angular calibration of a macroscopic vision system (section 3); and the analysis of angular measurement results obtained in the STT production process (section 4). The calibration measurement uncertainty is also evaluated and compared with the variability of the angular deviations found in a large sample of measured STT's and conclusions are drawn about the suitability of the applied quality control procedure.

2. STT MATHEMATICAL MODELS

The 10 strain measurements obtained with the STT, ε_i, (where i represents the strain gauge number) are used to determine the six stress tensor components (σ_x, σ_y, σ_z, τ_{xy}, τ_{xz}, τ_{yz}) through the Least Squares Method (LSM), based on the following equations:

$$E \cdot \varepsilon_1 = A \cdot \sigma_x + B \cdot \sigma_y + C \cdot \sigma_z + D \cdot \tau_{yz}, \quad (1)$$

$$E \cdot \varepsilon_2 = F \cdot \sigma_x + F \cdot \sigma_y + G \cdot \sigma_z + D_2 \cdot \tau_{yz} - D_2 \cdot \tau_{xz} + H_1 \cdot \tau_{xy}, \quad (2)$$

$$E \cdot \varepsilon_3 = I \cdot \sigma_x + J \cdot \sigma_y + L \cdot \sigma_z - D_3 \cdot \tau_{xz}, \quad (3)$$

$$E \cdot \varepsilon_4 = F \cdot \sigma_x + F \cdot \sigma_y + G \cdot \sigma_z - D_2 \cdot \tau_{yz} - D_2 \cdot \tau_{xz} - H_1 \cdot \tau_{xy}, \quad (4)$$

$$E \cdot \varepsilon_5 = A \cdot \sigma_x + B \cdot \sigma_y + C \cdot \sigma_z - D_1 \cdot \tau_{yz}, \quad (5)$$

$$E \cdot \varepsilon_6 = M \cdot \sigma_x + N \cdot \sigma_y + Q \cdot \sigma_z + H_2 \cdot \tau_{xy}, \quad (6)$$

$$E \cdot \varepsilon_7 = F \cdot \sigma_x + F \cdot \sigma_y + G \cdot \sigma_z - D_2 \cdot \tau_{yz} - D_2 \cdot \tau_{xz} + H_1 \cdot \tau_{xy}, \quad (7)$$

$$E \cdot \varepsilon_8 = I \cdot \sigma_x + J \cdot \sigma_y + L \cdot \sigma_z + D_3 \cdot \tau_{xz}, \quad (8)$$

$$E \cdot \varepsilon_9 = F \cdot \sigma_x + F \cdot \sigma_y + G \cdot \sigma_z + D_2 \cdot \tau_{yz} + D_2 \cdot \tau_{xz} - H_1 \cdot \tau_{xy}, \quad (9)$$

$$E \cdot \varepsilon_{10} = M \cdot \sigma_x + N \cdot \sigma_y + Q \cdot \sigma_z - H_2 \cdot \tau_{xy}, \quad (10)$$

where the values of A, B, C, D_1, D_2, D_3, F, G, H_1, H_2, I, J, L, M, N, Q depend on the rock's Poisson ratio and STT dimensional, geometrical and material properties [1].

Both the rock's modulus of elasticity, E, and corresponding Poisson's ratio, ν, are determined by laboratorial mechanical testing of a STT drill core using an biaxial pressure chamber with a 15 MPa range. This equipment allows applying a stress state characterized by $\sigma_x = \sigma_y = \sigma$ and $\tau_{xy} = \tau_{xz} = \tau_{yz} = 0$, so that the previous equations (1 to 10) can be written as

$$E \cdot \varepsilon_1 = E \cdot \varepsilon_5 = (0{,}306633 - 1{,}766620 \cdot \nu) \cdot \sigma, \quad (11)$$

$$E \cdot \varepsilon_2 = E \cdot \varepsilon_4 = E \cdot \varepsilon_7 = E \cdot \varepsilon_9 = (1{,}605554 - 0{,}778010 \cdot \nu) \cdot \sigma, \quad (12)$$

$$E \cdot \varepsilon_3 = E \cdot \varepsilon_8 = (2{,}101697 - 0{,}400394 \cdot \nu) \cdot \sigma, \quad (13)$$

$$E \cdot \varepsilon_6 = E \cdot \varepsilon_{10} = (2{,}408330 - 0{,}167014 \cdot \nu) \cdot \sigma. \quad (14)$$

This system of equations can also be solved by the LSM using, at least, two equations.

The LSM provides, in both cases (state of stress and rock mechanical properties), estimates for the unknown variables and analytical solutions for the corresponding covariance matrices.

3. ANGULAR TRACEABILITY OF THE MACROSCOPIC VISION SYSTEM

3.1. Main elements of the traceability chain

A set of angle block gauges (Kolb & Baumann, serial number 06189) with 13 metallic pieces with nominal values of 10'', 30'', 1', 2', 3', 10', 30', 1º, 2º, 3º, 10º, 30º and 60º, was used for the vision system calibration, as shown in Fig. 4.

SI traceability to primary angular standards was obtained through calibration to Eμmetron (accredited by DAkkS, reference D-K-15151-01-00, in accordance with the DIN EN ISO/IEC 17025 framework). The maximum value of the declared 95% measurement expanded uncertainty of the angular block gauges is 0,000 8º.

Fig. 4. Angular block gauges (on the left) used for the calibration of the macroscopic vision system (on the right).

The vision system (Mitutoyo, model QV-X302P1L-C), used by the LNEC's Applied Metrology Laboratory for the angular measurement in STT's, has a dimensional measurement range of (300 mm × 200 mm × 200 mm) with a resolution of 0,1 µm. The overall dimensional accuracy [5] ranges from 1,5 µm up to 3,2 µm. Regarding the angular measurements, the resolution is 0,000 1º, but no indication is given on the angular measurements accuracy.

3.2. Calibration procedure

The calibration procedure considers the evaluation of the angular accuracy in five positions (1 to 5) of the vision system table. The set of angular block gauges was used for each position and readings were taken for both surfaces (A and B) presented in Fig. 5.

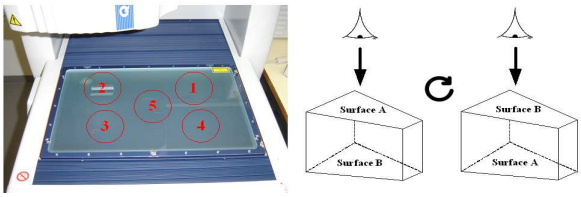

Fig. 5. Angular block gauges placement in the vision system table (on the left) and observed surfaces of the angular block gauges (on the right).

All readings were obtained using white light illumination (with a 15% intensity level) in order to optimize the image contrast (close to a binary image), and image points along the observed angular block gauge edges were obtained using the vision system software. In the next step, virtual lines were built using those points, defining the angular block surface (A or B), from which the α-angles were measured by computation (Fig. 6).

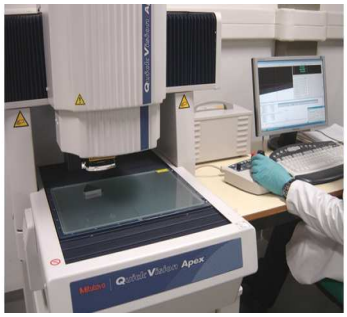

Fig. 6. Angular calibration of the macroscopic vision system.

Tests were carried out to estimate the calibration repeatability, complying with air temperature and relative humidity requirements defined for dimensional metrology (20 ºC ± 1 ºC and < 65% rh, respectively). One test was performed using the maximum magnification capability of the vision system (×15 for test #3) while the other two (tests #1 and #2) were performed with minimum magnification of ×2,5.

3.3. Results

The results obtained from the calibration of macroscopic vision system, considering different block gauge surfaces and observation positions are shown in Figures 7 and 8, respectively.

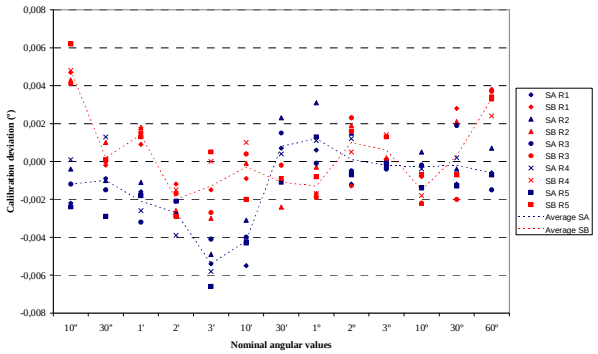

Fig. 7. Calibration deviations obtained for different observed block gauge surfaces (S) and table regions (R) – test #2 (×2,5).

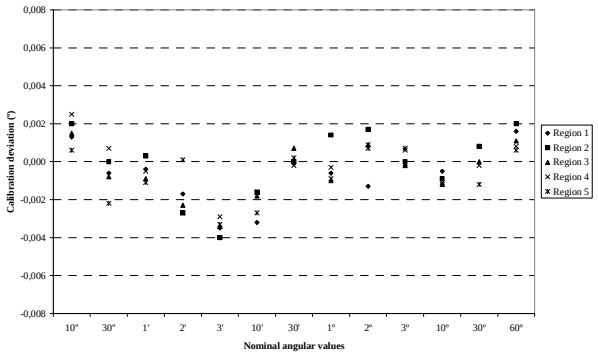

Fig. 8. Average calibration deviations obtained for different table regions – test #2 (×2,5).

The calibration deviations obtained (Fig. 7) were comprised between ± 0,006º. The higher deviations were found at angles nominal values of 10" and 3'. Between the angles of 30' to 30º, the calibration deviations were centred on a null value and showed reduced differences between observed gauge block surfaces. A maximum average difference of 0,006º was found for the 10" nominal value.

Regarding the influence of the observation position (Fig. 8), the dispersion of average calibration deviations had values from 0,000 7º (for a nominal value of 10º) to 0,003º (obtained for the angle of 2º). However, in a global view, results do not differ significantly between testing regions and, in addition, the central region (5) is usually the main observation region for angular measurements in STT's, making this uncertainty component less relevant for the angular measurement accuracy.

A cyclic variation of the average calibration deviations (between -0,004º and 0,002º) is noticed on Fig. 8, which can be explained by the air thermal variation in the laboratory (by correlation of values), taking into account the adopted calibration procedure (observation sequence from position 1 to 5 using the same angular block, starting with the 10" block and ending with the 60º block).

Figure 9 shows the results related to the evaluation of calibration repeatability, namely, the sample experimental standard deviations obtained for all the performed tests and angular block gauge surfaces A and B. A maximum standard deviation value of 0,002 5º was obtained for the 3' angular block.

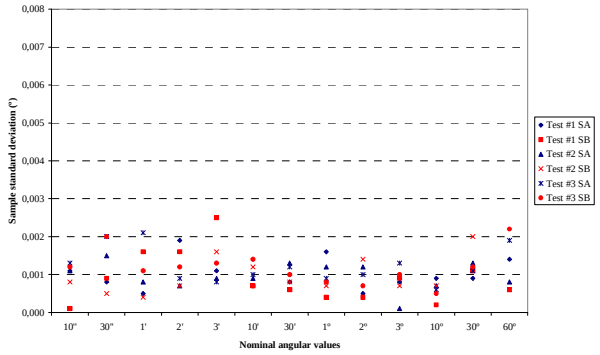

Fig. 9. Repeatability results.

Figure 10 shows the average calibration deviations obtained in all the performed tests, in order to evaluate the effect of magnification in the obtained results.

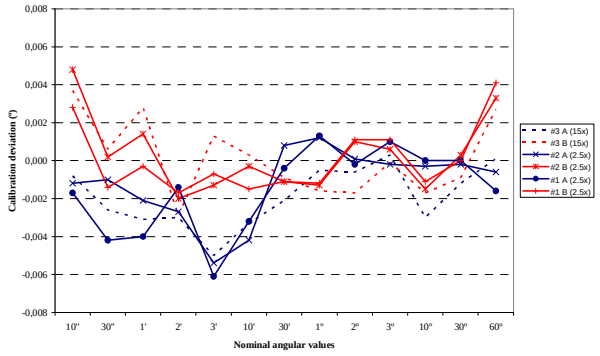

Fig. 10. Magnification effect on the calibration deviations.

The deviations obtained have similar magnitudes, however, a maximum absolute difference of 0,003º was observed between calibrations performed with different magnifications, for example, between tests #2 and #3 (surface A) for the 10º nominal value.

In addition to other sources of uncertainty, these experimental results were used for the quantification of the calibration measurement uncertainty according to the ISO GUM [6]. Table 1 presents the uncertainty sources identified in the calibration process and their probability distribution functions and the related measurement uncertainties.

Table 1. Uncertainty budget for the calibration of the macroscopic vision system.

Uncertainty source	**Probability distribution function**	**Measurement standard uncertainty contribution**
Calibration of the angular block gauges	Gaussian	0,000 4º
Drift between calibrations	Triangular	0,000 5º/√6 = 0,000 2º
Resolution of the vision system	Rectangular	0,000 05º/√3 = 0,000 03º
Variation due to block gauges surfaces	Rectangular	0,006º/√3 = 0,003 5º
Spatial variation (observation table)	Rectangular	0,003º/√3 = 0,001 7º
Repeatability	Gaussian	0,002 5º
Thermal influence	Rectangular	0,004º/√3 = 0,002 3º
Magnification	Rectangular	0,003º/√3 = 0,001 7º

Based on the presented values, the combined measurement standard uncertainty is equal to 0,005 5º. The 95% measurement expanded uncertainty of 0,011º was obtained using an expansion factor of 2,01 (for 52 degrees of freedom).

The results enhanced as main contribution for the measurement uncertainty the angular variation due to the observation of different surfaces of the angular block with a contribution of, approximately, 40% to the combined uncertainty. This uncertainty component is followed by the repeatability and the thermal influence, each one with an individual contribution of nearly 20% to the combined uncertainty.

The magnification effects as well as the spatial variation related to the observation table have a minor contribution (10% for each mentioned uncertainty component) to the final angular uncertainty value. The remaining uncertainty components (calibration of the angular blocks, drift between calibrations and resolution of the vision system) showed residual contributions (lower than 0,5%) to the obtained angular measurement uncertainty.

These results show that a calibration accuracy enhancement can be achieved by a more demanding thermal control of the laboratorial environment, in order to reduce the thermal influence uncertainty component, and by performing measurements in the same region of the observation table (usually the central region) and using the same optical magnification.

The instrumental angular accuracy of the macroscopic vision system of 0,013º can be obtained combining the calibration expanded uncertainty (0,011º) and the uncertainty related to the maximum calibration deviation (0,006º) systematic effect (by adopting a rectangular probability distribution with an expanded measurement uncertainty of 0,0069º).

4. STT PRODUCTION QUALITY CONTROL

4.1. Angular measurement procedure

The quality control procedure developed has six steps:

(i) visual analysis of the first group of strain gauges 2 and 3 (strain gauges identification shown on Fig. 3);

(ii) definition of the border lines related to the corresponding STT generatrices;

(iii) determination of the virtual middle line, parallel to the two border lines, defining the virtual STT axis;

(iv) definition of the orientation line between reference markings on the strain gauges, as shown in Fig. 11;

(v) perform the angular measurement between the orientation line and the virtual STT axis;

(vi) repeat all the steps for each of the remaining three groups of strain gauges (4-5, 6-7-8 and 9-10-1) accordingly to their geometrical arrangement.

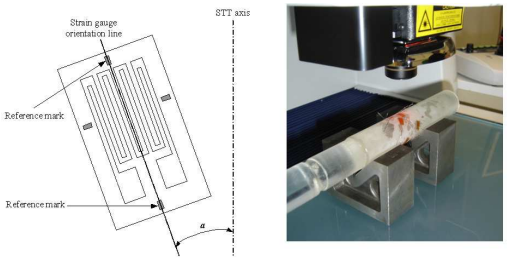

Fig. 11. Schematic representation of the angular measurement in a STT strain gauge (on the left) and real measurement (on the right).

4.2. Measurement results

This section presents the α-angle measurement results with respect to the STT production process, considering a sample of 28 instruments. The results are presented in Figures 12 to 15 (time scale) and in Figures 16 to 19 (angular deviations histograms) according to the strain gauges nominal value for the α-angle (69,1º , 35,3º , 20,9º and 0º, respectively).

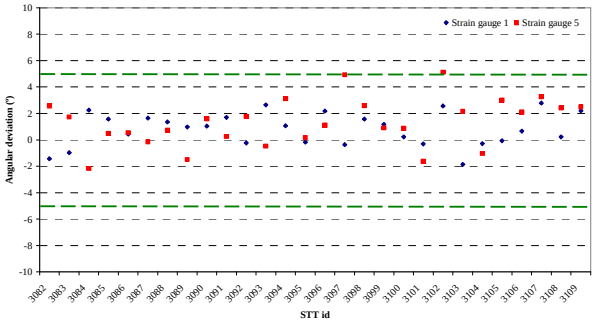

Fig. 12. Angular deviations for STT strain gauges 1 and 5 (69,1º nominal angle value).

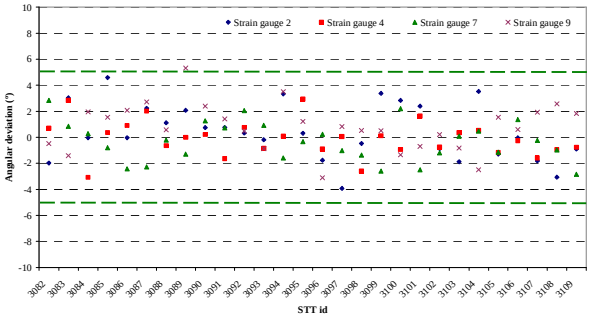

Fig. 13. Angular deviations for STT strain gauges 2, 4, 7 and 9 (35,3º nominal angle)

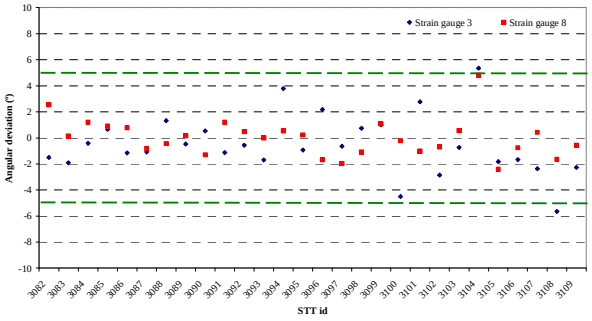

Fig. 14. Angular deviations for STT strain gauges 3 and 8 (20,9º nominal angle value).

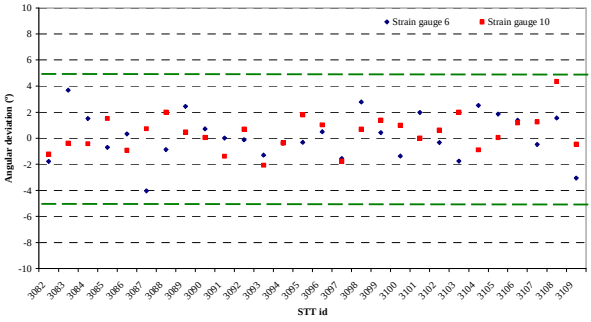

Fig. 15. Angular deviations for STT strain gauges 6 and 10 (0º nominal angle value).

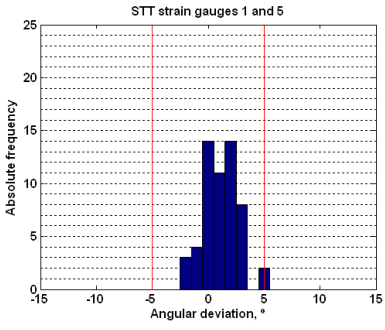

Fig. 16. Angular deviations histogram (69,1º nominal angle value).

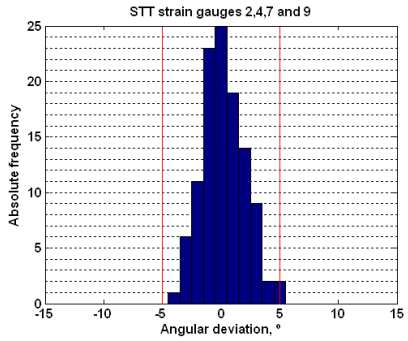

Fig. 17. Angular deviations histogram (35,3º nominal angle value).

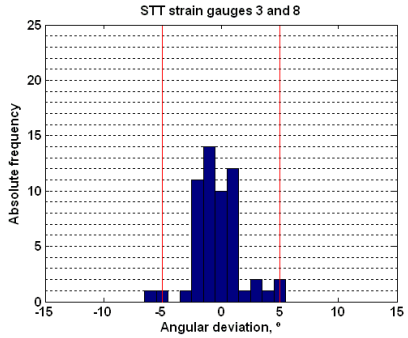

Fig. 18. Angular deviations histogram (20,9º nominal angle value).

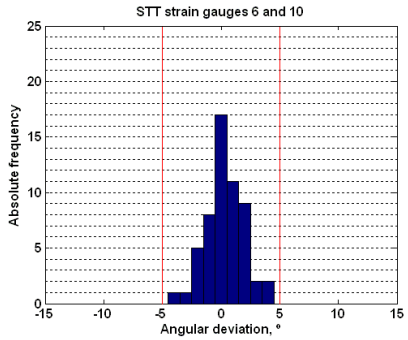

Fig. 19. Angular deviations histogram (0º nominal angle value).

The results show that a compliance of the angular measurements with a tolerance of ±5º is generally achieved (limits expressed in the figures by the horizontal green lines – time scale – and vertical red lines in the histograms). The analysis of the angular estimation dispersion related to the STT production process (the sample experimental standard deviation had a variation between 1,2º and 2,3º, depending on the measured strain gauge) shows that they are 100 times higher than the vision system angular accuracy level (0,013º).

Although the mean angular deviations are close to zero, some angular deviation values were found to be quite close to the tolerance limits which bring up the possibility of rejecting some strain gauges angular orientations with an increase of the dimension of observed STT sample.

Regarding the type of distribution for the output, Figure 17 shows a histogram with a geometrical shape and parameters characteristic of a Gaussian probability distribution. In the remaining histograms (Figures 16, 18 and 19) the Gaussian shape is not observed, possibly explained because of the lower dimension of the angular deviation samples (related to only two sets of strain gauges), which are two times smaller than the sample presented on Fig. 17 (related to four sets of strain gauges).

5. CONCLUSIONS

The use of SI traceable angular block gauges for the calibration of a macroscopic vision system was considered adequate for the purpose of the evaluation and quality control requirements related to the measurement of the α-angle of strain gauges in STT production. The instrumental accuracy level of 0,013º is acceptable when compared with quality control tolerances (±5º), thus being able to validate the use of a macroscopic vision system as a reference standard for the calibration of other types of angular gauges, namely, working angular standards, 90º squares and universal bevel protractors, where the target uncertainty (0,033º) may usually be obtained from ⅓ of an angular resolution equal to 0,1º (according to an accepted rule of thumb among metrologists).

Future work will be dedicated to measurement uncertainty propagation of the α-angle dispersion in STT's and its impact on the state of stress quantity which is obtained from complex and multivariable mathematical model. This will allow us to determine if the mentioned angular tolerance is acceptable for the required metrological quality (quantified by measurement uncertainty) of the state of stress quantity and if production efforts must be undertaken in order to comply with a more demanding angular tolerance interval (lower than ±5º).

Other important uncertainty components, namely, temperature compensation and correlation between input quantities (originated by the use of the same STT for field strain measurements and for the laboratorial determination of the rock's elasticity modulus and Poisson's ratio) must also be evaluated in this process. The effect of redundant strain measurements (from six to ten strain gauges) and its influence in the stress measurement accuracy will also be investigated.

REFERENCES

[1] J. L. Pinto, *A New Type of Apparatus to perform Stress Tensor Tube (STT) Tests*, LNEC Report 108/90-NFR, National Laboratory for Civil Engineering (LNEC), Lisbon, 1990.

[2] M. Rocha, *Mechanical Behaviour of Rock Foundations in Concrete Dams*, National Laboratory for Civil Engineering (LNEC), Lisbon, 1965.

[3] C. Demant, B. Streicher-Abel, P. Waszkewitz, *Industrial Image Processing: Visual Quality Control in Manufacturing*, Springer Verlag, Berlin, 1999.

[4] T. Coveney, *Dimensional Measurement using Vision Systems*, Measurement Good Practice Guide No. 39 - Issue 2, National Physical Laboratory (NPL), Teddington, 2014.

[5] *Mitutoyo GB-17001 Measuring Instrument Catalog 2012/2013*, Mitutoyo Europe GmbH, Neuss, May 2012.

[6] Evaluation of measurement data - Guide to the expression of Uncertainty in Measurement, Joint Committee for Guides in Metrology (JCGM), September 2008.